
Towards Deepening Graph Neural Networks: A GNTK-based Optimization Perspective

Wei Huang *

University of Technology Sydney, Australia
wei.huang-6@student.uts.edu.au

Yayong Li *

University of Technology Sydney, Australia
yayong.li@student.uts.edu.au

Weitao Du *

Northwestern University, USA
weitao.du@northwestern.edu

Richard Yi Da Xu

University of Technology Sydney, Australia
YiDa.Xu@uts.edu.au

Jie Yin

The University of Sydney, Australia
jie.yin@sydney.edu.au

Ling Chen

University of Technology Sydney, Australia
ling.chen@uts.edu.au

Miao Zhang

Monash University, Australia
miaozhang1991@gmail.com

Abstract

Graph convolutional networks (GCNs) and their variants have achieved great success in dealing with graph-structured data. However, it is well known that deep GCNs suffer from the over-smoothing problem, where node representations tend to be indistinguishable as more layers are stacked up. The theoretical research to date on deep GCNs has focused primarily on expressive power rather than trainability, an optimization perspective. Compared to expressivity, trainability attempts to address a more fundamental question: given a sufficiently expressive space of models, can we successfully find a good solution by gradient descent-based optimizer? This work fills this gap by exploiting the Graph Neural Tangent Kernel (GNTK), which governs the optimization trajectory under gradient descent for wide GCNs. We formulate the asymptotic behaviors of GNTK in the large depth, which enables us to reveal the dropping trainability of wide and deep GCNs at an exponential rate in the optimization process. Additionally, we extend our theoretical framework to analyze residual connection-resemble techniques, which are found to be only able to mildly mitigate the exponential decay of trainability. To overcome the exponential decay problem more fundamentally, we propose Critical DropEdge, a connectivity-aware and graph-adaptive sampling method, inspired by our theoretical insights on trainability. Experimental evaluation consistently confirms using our proposed method can achieve better results compared to relevant counterparts with both infinite-width and finite-width.

1 Introduction

Recently, Graph Convolutional Networks (GCNs) have shown incredible abilities to learn node or graph representations and achieved superior performances for various downstream tasks, such as

*Equal contribution.

node classifications [19, 37, 11], graph classifications [39, 8, 24, 45], and link predictions [20], etc. However, most GCNs achieve their best with a shallow depth, e.g., 2 or 3 layers, and their performance on those tasks would promptly degrade as the number of layers grows. Towards this phenomenon, research attempts have been made to deepen understanding of current GNN architectures and their expressive power. [27] showed that GCN is a special form of Laplacian smoothing, which mixes node representations with nearby neighbors. This mechanism potentially poses the risk of *over-smoothing* as more layers are stacked together, where node representations tend to be indistinguishable from each other. [31] investigated the expressive power of GNNs using the asymptotic behaviors as the layer goes to infinity. They proved that under certain conditions, the expressive power of GCN is determined by the topological information of the underlying graphs inherent in the graph spectra.

However, it remains elusive how to theoretically understand why deepen GCNs fail to optimize. Existing theoretical investigations [39, 31] on GNNs mainly focus on expressivity which measures how complex the function a network can represent. Exploring expressiveness is theoretically convenient, but the corresponding conditions may be broken during the gradient training process, thus leading to inconsistencies between theoretical conclusions and results of trained networks [10]. Compared to the expressivity, trainability attempts to address a more difficult but fundamental perspective of neural networks: how effective a network can be optimized via gradient descent. The advantage of studying trainability is that we can directly know whether the graph neural network can be successfully trained under certain conditions, and to what extent. We are therefore inspired to ask:

- *Can we theoretically characterize the trainability of graph neural networks with respect to depth, thus understanding why deep GCNs fail to generalize?*
- *Can we further design an algorithm to deepen GCNs benefit from our theoretical investigation?*

Our answers are yes to both questions. We resort to the infinitely wide multi-layer GCN. The research on infinitely-wide networks can be traced back to the seminal work of [30], which showed the one hidden layer networks with random weights at initialization (without training) are Gaussian Processes (GPs) in the infinite width limit. Later, the connection between GPs and multi-layer infinitely-wide networks with Gaussian initialization [22, 29] and orthogonal weights [16] was reported. Recent trends in Neural Tangent Kernel (NTK) have led to a proliferation of studies on the optimization and generalization of infinitely (ultra)-wide networks. In particular, [18] made a groundbreaking discovery that gradient descent training in the infinite width limit can be captured by an NTK. [4] formulated Graph Neural Tangent Kernel (GNTK) for infinitely-wide GNNs and shed light on theoretical guarantees for GNN. Prior to the discovery of GNTK, there was little understanding of the non-convexity of graph neural networks, which is analytically intractable. In the learning regime of GCN governed by GNTK, the optimization becomes an almost convex problem, making GNTK a promising method to study the trainability of deep GCNs.

In this work, we leverage the GNTK techniques of infinitely-wide networks to investigate whether ultra-wide GCNs are trainable in the large depth. In particular, we formulate the large-depth asymptotics behavior of the GNTK, illuminated by innovative works on deep networks [12, 38], through which we can analyze the optimization properties. We further extend our theoretical framework to residual connection-like techniques and show that these techniques can only help slow down the exponential decay of trainability to some extent, but lack the ability to overcome the problem thoroughly. Our contributions are as follows:

- To our best knowledge, we are the first to investigate the trainability of deep GCNs through GNTK. We prove that all elements of a GNTK matrix regarding a pair of graphs converge exponentially to the same value, making the GNTK matrix singular in the large depth. We thus establish a corollary that the trainability of ultra-wide GCNs exponentially collapses on node classification tasks.
- We apply our theoretical analysis to the residual connection-resemble techniques for GCNs. Our theory shows that residual connection can, to some extent, slow down the exponential decay rate, but can not fundamentally solve the exponential decay problem. This result can be used to explain to what extent the recent residual connection-resemble method works.
- Our theoretical framework provides comprehensive guidance for the development of deep GCNs. We propose an edge-based sampling method, named Critical DropEdge, to overcome the exponential decay of trainability. This graph-adaptive and connectivity-aware method

is easy to implement in both finite-width and infinite-width GNNs. Our experiments show using the proposed method can outperform counterparts in the large depth.

2 Background

We first review the results of infinitely-wide neural networks at initialization. Then we introduce the Neural Tangent Kernel, making a connection to trainability. Finally, we introduce Graph Convolutional Networks along with our setup and notation.

2.1 Infinitely-wide Networks at Initialization

We begin by considering a fully-connected network of depth L of widths m_l in each layer. The weight and bias in the l -th layer are denoted by $W^{(l)} \in \mathbb{R}^{m_l \times m_{l-1}}$ and $b^{(l)} \in \mathbb{R}^{m_l}$. Letting the pre-activations be given by $h_i^{(l)}$. Then the information propagation in this network is governed by,

$$h_i^{(l)} = \frac{\sigma_w}{\sqrt{m_l}} \sum_{j=1}^{m_l} W_{ij}^{(l)} \phi(h_j^{(l-1)}) + \sigma_b b_i^{(l)} \quad (1)$$

where $\phi : \mathbb{R} \rightarrow \mathbb{R}$ is the activation function, σ_w and σ_b define the variance scale of the weights and biases respectively. Given the parameterization that weights and biases are randomly generated by i.i.d. normal distribution, i.e., $W_{ij}^{(l)}, b_i^{(l)} \sim \mathcal{N}(0, 1)$, the pre-activations are Gaussian distributed in the infinite width limit as $m_1, m_2, \dots, m_{L-1} \rightarrow \infty$. This results from the central limit theorem (CLT). Consider a dataset $X \in \mathbb{R}^{n \times m_0}$ of size $n = |X|$, the covariance matrix of Gaussian process kernel (GPK) regarding infinitely-wide network is defined by $\Sigma^{(l)}(x, x') = \mathbb{E}[h_i^{(l)}(x)h_i^{(l)}(x')]$. According to the signal propagation Equation (1), the covariance matrix or Gaussian Process kernel with respect to layer can be described by a recursion relation, $\Sigma^{(l)}(x, x') = \sigma_w^2 \mathbb{E}_{h \sim \mathcal{N}(0, \Sigma^{(l-1)})}[\phi(h(x))\phi(h(x'))] + \sigma_b^2$.

The mean-field theory is a paradigm that studies the limiting behavior of GPK, which is a measure of expressivity for networks [32, 35]. In particular, expressivity describes to what extent two different inputs can be distinguished. The property of evolution for expressivity $\Sigma^{(l)}(x, x')$ is determined by how fast it converges to its fixed point $\Sigma^*(x, x') \equiv \lim_{l \rightarrow \infty} \Sigma^{(l)}(x, x')$. It is shown that in almost the entire parameter space spanned by hyper-parameters σ_w and σ_b , the evolution exhibits a dramatic convergence rate formulated by an exponential function except for a critical line known as the *edge of chaos* [32, 35, 42]. Consequently, an infinitely-wide network loses its expressivity exponentially in most cases while retaining the expressivity at the edge of chaos. Given this reason, we focus on the edge of chaos in this work. In particular, we set the value of hyper-parameters to satisfy, $\sigma_w^2 \int \mathcal{D}_z [\phi'(\sqrt{q^*}z)]^2 = 1$, where q^* is the fixed point of diagonal elements in the covariance matrix, and $\int \mathcal{D}z = \frac{1}{\sqrt{2\pi}} \int dz e^{-\frac{1}{2}z^2}$ is the measure for a normal distribution. For the ReLU activation, edge of chaos requires $\sigma_w^2 = 2$ and $\sigma_b^2 = 0$.

2.2 Neural Tangent Kernel and Trainability

Most studies on infinitely-wide networks through mean-field theory [32, 35] have focused solely on initialization without training. [18] took a step further by considering the infinitely-wide network trained with gradient descent. Let η be the learning rate, and \mathcal{L} be the loss function. The dynamics of gradient flow for parameters $\theta = \text{vec}(\{W_{ij}^{(l)}, b_i^{(l)}\}) \in \mathbb{R}^{(\sum_l m_l(m_{l-1}+1)) \times 1}$, the vector of all parameters, is given by,

$$\frac{\partial \theta}{\partial t} = -\eta \nabla_{\theta} \mathcal{L} = -\eta \nabla_{\theta} f_t(X)^T \nabla_{f_t(X)} \mathcal{L} \quad (2)$$

Then the dynamics of output functions $f(X) = \text{vec}(f(x)_{x \in X}) \in \mathbb{R}^{nm_L \times 1}$ follow,

$$\frac{\partial f_t(X)}{\partial t} = \nabla_{\theta} f_t(X) \frac{\partial \theta}{\partial t} = -\eta \Theta_t(X, X) \nabla_{f_t(X)} \mathcal{L} \quad (3)$$

where the NTK at time t is defined as,

$$\Theta_t(X, X) \equiv \nabla_{\theta} f_t(X) \nabla_{\theta} f_t(X)^T \in \mathbb{R}^{nm_L \times nm_L} \quad (4)$$

In a general case, the NTK varies with the training time, thus providing no substantial insight into the convergence property of neural networks. Interestingly, as shown by [18], the NTK converges to an explicit limiting kernel and does not change during training in the infinite width limit. This leads to a simple but profound result in the case of an MSE loss, $\mathcal{L} = \frac{1}{2} \|f_t(X) - Y\|_F^2$, where Y is the label regarding the input X ,

$$f_t(X) = (I - e^{-\eta\Theta_\infty(X,X)t})Y + e^{-\eta\Theta_\infty(X,X)t}f_0(X) \quad (5)$$

where Θ_∞ is the limiting kernel. This is the solution of an ordinary differential equation. As the training time t tends to infinity, the output function fits the label very well, i.e., $f_\infty(X) = Y$. As proved by [12] (Lemma 1), the network is trainable only if $\Theta_\infty(X, X)$ is non-singular. Quantitatively, the condition number $\kappa \equiv \lambda_{\max}/\lambda_{\min}$ can be a measure of trainability as confirmed by [38].

2.3 Graph Convolutional Networks

We define an undirected graph as $G = (V, E)$, where V is a collection of nodes while E is a set of edges. We denote the number of nodes in graph G by $n = |V|$. The node features are denoted as $h_v \in \mathbb{R}^d$ for each $v \in V$, with d being the dimension of node features. In this work, we develop our theory towards understanding the trainability of GCNs on node classification tasks.

GCNs iteratively update node features through aggregating and transforming the representation of their neighbors. Figure 3 in Appendix A illustrates an overview of the information propagation in a general GCN. We define a propagation unit to be the combination of a R -layer MLP and one aggregation operation. We use subscript (r) to denote the layer index of MLP in each propagation unit and use superscript (l) to indicate the index of aggregation operation, which is also the index of the propagation unit. L is the total number of propagation units. Specifically, the node representation propagation in GCNs through a multi-layer perceptron (MLP) follows the expression,

$$h_{(0)}^{(l)}(u) = \frac{1}{|\mathcal{N}(u)| + 1} \sum_{v \in \mathcal{N}(u) \cup u} h_{(R)}^{(l-1)}(v) \quad (6)$$

$$h_{(r)}^{(l)}(u) = \frac{\sigma_w}{\sqrt{m}} W_{(r)}^{(l)} \phi(h_{(r-1)}^{(l)}(u)) + \sigma_b b_{(r)}^{(l)} \quad (7)$$

where $W_{(r)}^{(l)} \in \mathbb{R}^{m_l \times m_{l-1}}$ and $b_{(r)}^{(l)} \in \mathbb{R}^{m_l}$ are the learnable weights and biases respectively, ϕ is the activation function, $\mathcal{N}(u)$ is the neighborhood of node u , and $\mathcal{N}(u) \cup u$ is the union of node v and its neighbors. Equation (6) describes the node feature aggregation operation among its neighborhood according to a GCN variant [11]. Equation (7) is a standard non-linear transformation with NTK-parameterization [18], where m is the width, i.e., number of neurons in each layer, σ_w and σ_b define the variance scale of the weights and biases. With regard to the activation function, we focus on both ReLU and tanh, which are denoted as $\phi(x) = \max\{0, x\}$ and $\phi(x) = \tanh(x)$ respectively. Without loss of generality, our theoretical framework can handle other common activations. By comparison, the GNTK work [4] only adopted ReLU activation.

3 Aggregation Provably Leads to Exponential Trainability Loss

3.1 GNTK Formulation

On the basis of the definition of NTK (Equation 4), we recursively formulate the propagation of GNTK in the infinite-width limit. Since the information propagation in a GCN is built on two operations: aggregation (Equation 6) and non-linear transformation (Equation 7), the corresponding formulas of GNTK are expressed as follows,

$$\Theta_{(0)}^{(l)}(u, u') = \frac{1}{|\mathcal{N}(u)| + 1} \frac{1}{|\mathcal{N}(u')| + 1} \sum_{v \in \mathcal{N}(u) \cup u} \sum_{v' \in \mathcal{N}(u') \cup u'} \Theta_{(R)}^{(l-1)}(v, v') \quad (8)$$

$$\Theta_{(r)}^{(l)}(u, u') = \Theta_{(r-1)}^{(l)}(u, u') \dot{\Sigma}_{(r)}^{(l)}(u, u') + \Sigma_{(r)}^{(l)}(u, u') \quad (9)$$

The two equations above correspond to the aggregation operation and MLP transformation respectively. To compute the GNTK with respect to the depth, the key step is to obtain the covariance

matrix $\Sigma_{(r)}^{(l)}(u, u') \equiv \mathbb{E}[h_{(r)}^{(l)}(u)h_{(r)}^{(l)}(u')]$. According to the CLT, the node representation $h_{(r)}^{(l)}(u)$ is Gaussian distributed in the infinite width limit. Applying this result to Equation (6) and (7) the resulting covariance matrix is composed of two parts,

$$\Sigma_{(0)}^{(l)}(u, u') = \frac{1}{|\mathcal{N}(u)| + 1} \frac{1}{|\mathcal{N}(u')| + 1} \sum_{v \in \mathcal{N}(u) \cup u} \sum_{v' \in \mathcal{N}(u') \cup u'} \Sigma_{(R)}^{(l-1)}(v, v') \quad (10)$$

$$\begin{aligned} \Sigma_{(r)}^{(l)}(u, u') &= \sigma_w^2 \mathbb{E}_{z_1, z_2 \sim \mathcal{N}(0, \tilde{\Sigma}_{(r-1)}^{(l)})} [\phi(z_1)\phi(z_2)] + \sigma_b^2 \\ \dot{\Sigma}_{(r)}^{(l)}(u, u') &= \sigma_w^2 \mathbb{E}_{z_1, z_2 \sim \mathcal{N}(0, \tilde{\Sigma}_{(r-1)}^{(l)})} [\dot{\phi}(z_1)\dot{\phi}(z_2)] + \sigma_b^2 \end{aligned} \quad (11)$$

The first equation results from the aggregation operation. Meanwhile, the second equation corresponds to the R -times non-linear transformations, where z_1, z_2 are drawn from a 2-dimensional Gaussian distribution of the previous MLP layer, and the variance $\tilde{\Sigma}_{(r-1)}^{(l)} \in \mathbb{R}^{2 \times 2}$ is across u, u' .

3.2 Trainability in the Large Depth

We aim to characterize the behavior of $\Theta_{(r)}^{(l)}(G) = \Theta_{(r)}^{(l)}(\mathcal{V}, \mathcal{V}) \in \mathbb{R}^{n \times n}$, where we denote $\mathcal{V} = [v_1, v_2, \dots, v_n]$, as the depth tends to infinity $l \rightarrow \infty$. From the GNTK formulation, both aggregation (Equation 8) and transformation (Equation 9) contribute simultaneously to the final limiting result. Taking them into consideration, we derive our theorem on the asymptotic behavior of infinitely-wide GCN in the large depth limit, which is as follows:

Theorem 1 (Convergence Rate of the GNTK). *If transition matrix $\mathcal{A}(G) \in \mathbb{R}^{n^2 \times n^2}$ is irreducible and aperiodic, with a stationary distribution vector $\vec{\pi}(G) \in \mathbb{R}^{n^2 \times 1}$, where $\tilde{\Theta}_{(0)}^{(l)}(G) = \mathcal{A}(G)\tilde{\Theta}_{(R)}^{(l-1)}(G)$ and $\tilde{\Theta}_{(r)}^{(l)}(G) \in \mathbb{R}^{n^2 \times 1}$ is the result of being vectorized. Then there exist constants $0 < \alpha < 1$ and $C > 0$, and constant vector $\vec{v}, \vec{v}' \in \mathbb{R}^{n^2 \times 1}$ depending on the number of MLP iterations R , such that $|\Theta_{(r)}^{(l)}(u, u') - \vec{\pi}(G)^T (Rl\vec{v} + \vec{v}')| \leq C\alpha^l$.*

The proof sketch follows a divide-and-conquer manner. In particular, we first analyze the network with the only aggregation and prove that $\mathcal{A}(G)$ is a Markov transition matrix. Then we formulate the behavior of MLP in the large depth based on [12]. Finally, we arrive at the final result by considering the two operations. We leave the complete proof in Appendix B.

In Theorem 1, we rigorously characterize the convergence properties of GNTK in the large depth limit. As depth goes to infinity, all elements in the GNTK converge to a unique quantity at an exponential rate. We thus have $\Theta_{(R)}^{(L)}(\mathcal{V}, \mathcal{V}) \approx \vec{\pi}(G)^T (RL\vec{v})\mathbf{1}_{n \times n}$ as $L \rightarrow \infty$, where $\mathbf{1}_{n \times n}$ is the $(n \times n)$ -dimensional matrix whose elements are one. The exponential convergence rate of $\Theta_{(R)}^{(L)}(\mathcal{V}, \mathcal{V})$ implies that the trainability of infinitely wide GCNs degenerate dramatically, as shown in following corollary.

Corollary 1 (Trainability of Ultra-Wide GCNs). *Consider a GCN of the form (6) and (7), with depth L , non-linear transformations number R , an MSE loss, and a Lipchitz activation $\phi(x)$, trained with gradient descent on a node classification task. Then the output function follows,*

$$f_t(\mathcal{V}) = e^{-\eta\Theta_{(R)}^{(L)}(\mathcal{V}, \mathcal{V})t} f_0(\mathcal{V}) + (I - e^{-\eta\Theta_{(R)}^{(L)}(\mathcal{V}, \mathcal{V})t}) \mathcal{Y}$$

where \mathcal{Y} is the label with respect to node \mathcal{V} . Then, there exists a positive integer L_0 such that, $\Theta_{(R)}^{(L)}(\mathcal{V}, \mathcal{V})$ is singular when $L > L_0$. Moreover, there exist a constant $C > 0$ such that for all $t > 0$, $\|f_t(\mathcal{V}) - \mathcal{Y}\| > C$.

According to the above corollary, as $L \rightarrow \infty$, the GNTK matrix will become a singular matrix. This would lead to a discrepancy between output $f_t(\mathcal{V})$ and label \mathcal{Y} , which means GNTK loses the ability to fit the label. Therefore, an ultra-wide GCN with a large depth cannot be trained successfully on node classification tasks.

4 Towards Deepening Graph Neural Networks

4.1 Theoretical Analysis on Residual Connection

We have characterized the trainability of vanilla GCNs through GNTKs and show that the trainability of ultra-wide GCNs drops at an exponential rate. Recently, considerable efforts have been made to deepen GCNs, of which residual connection-resemble techniques are widely applied to resolve the over-smoothing problem [25]. We apply our theoretical framework to analyze to what extent residual connection techniques could alleviate the trainability loss problem.

We first consider residual connection in aggregation, in which the propagation of the GNTK can be formulated as,

$$\vec{\Theta}^{(l)}(G) = (1 - \delta)\mathcal{A}(G)\vec{\Theta}^{(l-1)}(G) + \delta\vec{\Theta}^{(l-1)}(G), \quad (12)$$

where $0 < \delta < 1$, and $C > 0$. Taking Equation (12) as a new aggregation operation matrix, $\vec{\Theta}^{(l)}(G) = \tilde{\mathcal{A}}(G)\vec{\Theta}^{(l-1)}(G)$, where $\tilde{\mathcal{A}}(G) = (1 - \delta)\mathcal{A}(G) + \delta I$. We prove that $\tilde{\mathcal{A}}(G)$ is also a transition matrix with a greater second largest eigenvalue compared to the original matrix $\mathcal{A}(G)$.

Theorem 2 (Convergence rate for residual connection in aggregation). *Consider a GNTK of the form (12) with non-linear transformation of the form (7). Then with a stationary vector $\tilde{\pi}(G)$ for $\tilde{\mathcal{A}}(G)$, there exist constants $0 < \alpha < 1$ and $C > 0$, and constant matrix \vec{v} and \vec{v}' depending on R , such that $|\Theta_{(r)}^{(l)}(u, u') - \tilde{\pi}(G)^T(Rl\vec{v} + \vec{v}')| \leq C\alpha^l$. Furthermore, we denote the second largest eigenvalue of $\mathcal{A}(G)$ and $\tilde{\mathcal{A}}(G)$ as λ_2 and $\tilde{\lambda}_2$, respectively. Then, $\tilde{\lambda}_2 > \lambda_2$.*

The proof of theorem 2 can be found in Appendix C.1. This theorem implies a residual connection in aggregation can slow down the convergence rate, which is consistent with the empirical observations that residual connection-resemble methods can deepen GCNs.

Then we consider residual connection only applied on non-linear transformations (MLP). In this case, the recursive equation for the corresponding GNTK can be expressed as,

$$\Theta_{(r)}^{(l)}(u, u') = \Theta_{(r-1)}^{(l)}(u, u')(\Sigma_{(r)}^{(l)}(u, u') + 1) + \Sigma_{(r)}^{(l)}(u, u') \quad (13)$$

This formula is similar to the vanilla GNTK in the infinitely wide limit. Only an additional residual term appears according to the residual connection. It turns out that this term may not help slow down the convergence rate for non-linear transformation.

Theorem 3 (Convergence rate for GNTK with residual connection between transformations). *Consider a GNTK the form (8) and (13). If $\mathcal{A}(G)$ is irreducible and aperiodic, with a stationary distribution $\tilde{\pi}(G)$, then there exist constants $0 < \alpha < 1$ and $C > 0$, and constant matrix \vec{v} and \vec{v}' depending on R , such that, $|\Theta_{(r)}^{(l)}(u, u') - \tilde{\pi}(G)^T(Rl(1 + \frac{\sigma_w^2}{2})^{Rl}\vec{v} + \vec{v}')| \leq C\alpha^l$.*

The proof of the above theorem can be found in Appendix C.2. Theorem 3 demonstrates that adding residual connection in MLP cannot even reduce the convergence speed of trainability. Finally, we consider the residual connection applied to both aggregation and non-linear transformation simultaneously:

Corollary 2 (Convergence rate for GNTK with residual connection in aggregation and transformation). *Consider a GNTK of the form (12) and (13). If $\tilde{\mathcal{A}}(G)$ is irreducible and aperiodic, with a stationary distribution $\tilde{\pi}(G)$, there exist constants $0 < \alpha < 1$ and $C > 0$, and constant vectors $\vec{v}, \vec{v}' \in \mathbb{R}^{n^2 \times 1}$ depending on R , such that $|\Theta_{(r)}^{(l)}(u, u') - \tilde{\pi}(G)^T(Rl(1 + \frac{\sigma_w^2}{2})^{Rl}\vec{v} + \vec{v}')| \leq C\alpha^l$.*

4.2 A New Sampling Method: Critical DropEdge

Residual connection is a technique designed from a layer-wise perspective, but it has limited abilities to mitigate the exponential decay problem. To better solve the problem of trainability loss, we need to look deeper into the cause of the problem, which is the transition matrix corresponding to the aggregation operation. A necessary condition for matrix $\mathcal{A}(G)$ to be a probability transition matrix is that graph G is connected, which is a typical attribute for graphs used on both node and graph classification tasks. Therefore, breaking the connectivity condition is a promising direction. Interestingly, the critical percolation theory [17, 36] provides useful insights to better solve the exponential decay problem.

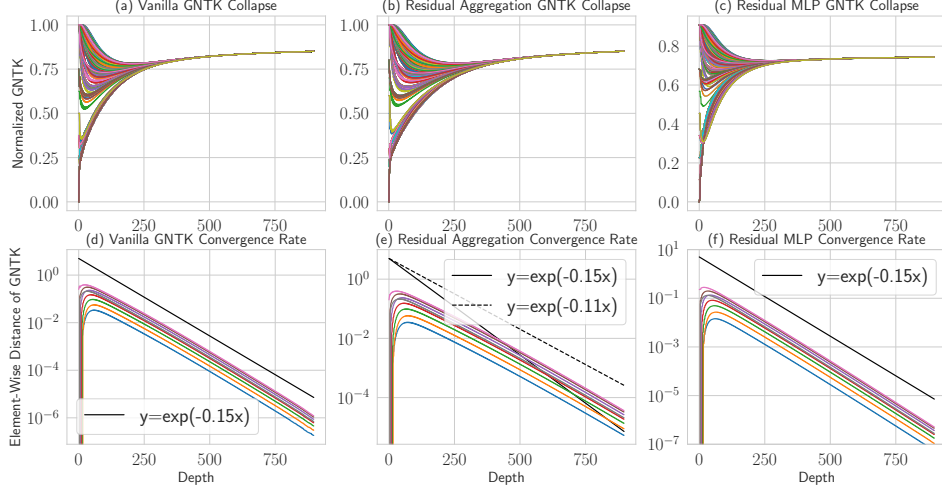


Figure 1: Convergence rate for the GNKT. (a,b,c) Element of the normalized (residual connection) GNKT as a function of depth that is defined as $Rl + r$. All elements tend to have the same value as depth grows. (d,e,f) The element-wise distance of the normalized (residual connection) GNKT as a function of the depth. The converge rate can be bounded by an exponential function $y = \exp(-0.15x)$ for vanilla and residual MLP GNKT, while the convergence rate for residual aggregation is bounded by $y = \exp(-0.11x)$.

On a finite complete graph of n nodes, there exist $E_t = n(n-1)/2$ edges between all pairs of nodes. A random graph \hat{G} is achieved by randomly and uniformly dropping some edges from the complete graph with the edge probability as $p = \frac{|E|}{E_t}$, where $|E|$ is the number of edges retained in the random graph. In this way, the critical percolation can be realized in the random graph with a critical edge probability $p_c = 1/(n-1)$ [6]. In the thermodynamic limit of $n \rightarrow \infty$, the critical random graph exhibits critical connectivity: the probability that there is an open path from some fixed point (say the origin) to a distance decreases polynomially:

Proposition 1 (Critical Connectivity in Random Graph [6]). *Suppose a random graph \hat{G} has n nodes with a constant edge probability p . (1) If $p < p_c$, then almost every random graph is such its largest component² has $O(\log n)$; (2) If $p > p_c$, the random graph has a giant component of $(1 - \alpha_p + o(1))n$, where $\alpha_p < 1$; (3) If $p = p_c$, then the maximal size of a component of almost every graph has order $n^{2/3}$.*

The proposition above implies that the information transforms in the critical random graph at a polynomial rate rather than an exponential rate, thus can solve the problem of exponentially dropping trainability. Inspired by this result, we design a graph-dependent and connectivity-aware sampling algorithm. In particular, given a graph G , we randomly drop some edges and retain the number of edges as $E_r = E_t \cdot p_c = n/2$, to approximate the critical graph. Note that a related work called DropEdge [33], which randomly removes a certain number of edges from the input graph. Different from them, our method fixes the edge preserving percentage as $\rho = E_r/|E| = \frac{|V|}{2|E|}$. On the contrary, DropEdge method may choose the edge probability as $p < p_c$ where information can only be passed to a distance of $O(\log n)$ in the graph, or $p > p_c$ in which the exponential trainability problem just exists. Our method is inspired by the critical percolation theory and thus it is named as Critical DropEdge.

5 Experiments

In this section, we illustrate empirically the theoretical results obtained in Section 3 and present the performance of the proposed Critical DropEdge on node classification. Details of these datasets are

²In graph theory, a component of an undirected graph is an induced subgraph in which any two vertices are connected to each other by paths.

summarized in Table 3 in Appendix D.1. We use a bioinformatics dataset (i.e., MUTAG) to verify the theoretical results for GNTK. The remaining three citation network datasets (i.e., Cora, Citeseer, and Pubmed) are used to verify the trainability of wide GCNs and the performance of the proposed Critical DropEdge on node classification tasks.

5.1 Convergence Results of GNTKs

Theorems 1, 2, and 3 provide a theoretical convergence rate for the (residual) GNTK. We demonstrate the corresponding numerical verification in Figure 1. We select a graph from the MUTAG dataset and generate the GNTK with ReLU activation, with $R = 3$, and $L = 300$. Figure 1 (a,b,c) show all elements of normalized GNTKs converge to an identical value as the depth goes larger. Figure 1 (d,e,f) further illustrate the convergence rate of the GNTK is exponential, as reflected by theorems. By comparing the convergence rate, we conclude that the residual connection in aggregation can slow down the convergence rate, which is consistent with Theorem 2.

5.2 Trainability of Wide GCNs

We further examine whether ultra-wide GCNs can be trained successfully on node classification. We conduct experiments on a GCN [19], where we apply a width of 1000 at each hidden layer and the depth ranging from 2 to 29. Figure 2 shows the training and test accuracy on various datasets after 300 training epochs. These results show the dramatic drop in both training and test accuracy as the depth grows, confirming that wide GCNs lose trainability significantly in the large depth on node classification as revealed by Corollary 1.

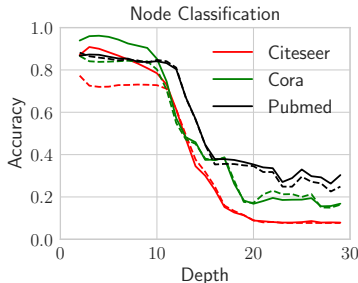


Figure 2: Train and test accuracy depending on the depth on different datasets. Solid and dashed lines are train and test accuracy respectively.

5.3 Evaluation of Critical DropEdge

We apply Critical DropEdge to both infinite-width and finite-width GCNs on node classification with a semi-supervised setting. For infinite-width GCNs, we consider two backbones: GCN [19] and JKNet [40], while we use three backbones (GCN, JKNet, IncepGCN [33]) for finite-width GCNs. The corresponding results for the infinite-width GCNs can be found in Appendix E.1. As for finite-width GCNs we use the hyper-parameter reported in [33] to obtain the results for DropEdge. On the other hand, we perform a random hyper-parameter search and fix the edge preserving percent as $\rho(G) = \frac{|V|}{2|E|}$ for C-DropEdge. Table 1 summarizes the performance on three citation network datasets with finite-width GCNs. In this table, we report the performance of GCNs with 4/8/16/32 layers and implementation details can be found in Appendix D.2. For each hyperparameter, we run 10 times and report the mean and standard variance. It is shown that C-DropEdge consistently outperforms vanilla and DropEdge counterparts, with both infinite-width and finite-width, especially when the model is deep. Besides, our C-DropEdge method can achieve smaller error bars, indicating that our method is more robust than DropEdge.

Finally, we perform an empirical study of whether the proposed drop rate value is indeed optimal or close to optimal to strengthen our results. To this end, we conducted experiments on dropping edges at various rates (sampling percent) and verified that the rate of Critical DropEdge can achieve the results closed to optimal, as shown in Table 2.

6 Related Work

Neural Tangent Kernel. NTKs are used to describe the dynamics of infinitely-wide networks during gradient descent training. In the infinite width limit, NTK converges to an explicit limiting kernel; besides, it stays constant during training, providing a convergence guarantee for over-parameterized networks [18, 23, 2, 43, 15, 1, 5, 48]. Besides, NTK has been applied to various architecture and brought a wealth of results, such as orthogonal initialization [16], convolutions [2], graph neural networks [4], attention [14], and see [44] for a summary. As for graph networks, GNTK helps us

Table 1: Comparison results of test accuracy (%) between C-DropEdge and DropEdge.

Dataset	Backbone	4-layer				8-layer		
		Finite	Original	DropEdge	C-DropEdge	Original	DropEdge	C-DropEdge
Cora	GCN	79.8 ± 1.1	80.4 ± 1.4	82.0 ± 1.2	73.2 ± 2.7	75.1 ± 2.4	77.3 ± 2.5	
	JKNet	81.1 ± 1.0	82.2 ± 0.7	82.5 ± 0.7	80.9 ± 1.2	82.0 ± 0.9	82.1 ± 0.5	
	IncepGCN	80.0 ± 0.9	80.6 ± 1.2	82.4 ± 0.5	78.6 ± 1.7	81.2 ± 1.3	82.3 ± 0.6	
Citeseer	GCN	61.2 ± 3.0	63.7 ± 2.5	69.0 ± 0.8	50.2 ± 5.7	52.8 ± 5.1	54.1 ± 5.9	
	JKNet	69.6 ± 1.2	70.2 ± 1.0	70.3 ± 0.7	70.7 ± 1.0	70.5 ± 1.1	70.8 ± 1.2	
	IncepGCN	69.4 ± 1.5	70.0 ± 1.0	70.8 ± 0.6	69.0 ± 1.2	70.8 ± 1.1	70.9 ± 0.5	
Pubmed	GCN	77.4 ± 0.7	77.6 ± 1.4	78.0 ± 0.4	57.2 ± 8.4	57.5 ± 6.1	58.9 ± 6.9	
	JKNet	76.5 ± 0.9	77.1 ± 1.1	77.4 ± 1.0	76.1 ± 1.4	76.6 ± 1.0	76.6 ± 0.9	
	IncepGCN	76.7 ± 1.7	77.4 ± 1.5	77.6 ± 1.1	77.5 ± 1.3	77.3 ± 1.2	77.9 ± 1.0	

Dataset	Backbone	16-layer			32-layer		
		Finite	Original	DropEdge	C-DropEdge	Original	DropEdge
Cora	GCN	36.3 ± 13.8	55.1 ± 5.2	58.5 ± 3.9	20.1 ± 2.4	22.1 ± 2.0	24.7 ± 1.8
	JKNet	79.9 ± 1.6	82.2 ± 0.7	82.4 ± 0.8	80.4 ± 1.4	82.1 ± 0.5	82.6 ± 0.9
	IncepGCN	78.7 ± 1.0	80.2 ± 1.3	82.0 ± 0.8	78.5 ± 1.8	80.9 ± 0.8	81.6 ± 0.9
Citeseer	GCN	30.8 ± 2.2	35.7 ± 1.9	36.6 ± 2.0	21.7 ± 3.0	23.1 ± 1.0	25.2 ± 0.9
	JKNet	69.2 ± 1.2	68.8 ± 1.6	69.5 ± 1.0	68.1 ± 2.3	69.9 ± 1.4	70.1 ± 0.6
	IncepGCN	68.4 ± 1.2	70.7 ± 1.0	71.0 ± 1.0	68.6 ± 1.9	70.2 ± 0.8	70.7 ± 0.9
Pubmed	GCN	39.5 ± 10.3	37.0 ± 9.6	42.6 ± 6.4	36.3 ± 8.4	37.4 ± 8.8	38.5 ± 6.1
	JKNet	76.6 ± 0.9	76.1 ± 0.8	76.9 ± 0.9	77.1 ± 0.8	77.0 ± 0.9	77.2 ± 1.0
	IncepGCN	76.5 ± 1.5	76.7 ± 1.3	77.2 ± 1.0	77.0 ± 1.4	77.2 ± 1.3	77.8 ± 1.0

Table 2: Comparison results of test accuracy between various drop rate. Critical drop rate for each dataset is marked as black font.

Rate	Cora		Citeseer			Pubmed		
	GCN-8	JKNet-4	Rate	GCN-4	IncepGCN-4	Rate	JKNet-16	IncepGCN-32
0.05	58.2 ± 19.6	82.0 ± 0.6	0.15	68.8 ± 1.2	70.1 ± 0.7	0.01	76.1 ± 1.8	75.5 ± 1.9
0.10	69.6 ± 14.4	82.1 ± 0.6	0.20	68.8 ± 1.1	70.6 ± 0.9	0.05	76.2 ± 1.5	76.1 ± 1.3
0.15	69.7 ± 12.5	82.2 ± 0.6	0.25	68.7 ± 0.8	70.5 ± 0.9	0.10	76.0 ± 1.4	76.8 ± 1.3
0.20	75.4 ± 4.0	82.5 ± 0.7	0.30	68.9 ± 0.8	70.5 ± 0.9	0.15	76.9 ± 0.9	77.0 ± 1.4
0.25	77.3 ± 2.5	82.5 ± 0.7	0.35	69.0 ± 0.8	70.8 ± 0.6	0.22	76.9 ± 0.9	77.8 ± 0.9
0.30	77.2 ± 2.7	82.2 ± 1.1	0.40	68.9 ± 0.9	70.5 ± 0.4	0.25	76.9 ± 1.1	75.8 ± 2.5
0.35	77.2 ± 2.8	81.7 ± 0.8	0.45	68.4 ± 1.7	70.1 ± 0.7	0.30	76.8 ± 1.1	77.1 ± 1.2
0.40	74.9 ± 5.7	81.4 ± 0.6	0.50	68.1 ± 0.9	70.2 ± 0.8	0.35	76.4 ± 1.2	77.6 ± 1.3
0.45	75.5 ± 6.4	81.7 ± 0.7	0.55	68.0 ± 1.0	70.3 ± 0.7	0.40	76.3 ± 1.3	77.6 ± 1.1

understand how GNN learn a class of smooth functions on graphs [4] and how GNN extrapolate differently from multi-layer perceptron [41].

Deep Graph Neural Networks. Since GNNs suffer from over-smoothing problem, a large and growing body of literature has made efforts deepening graph neural networks. There is a line of methods that resort to *residual connection* to keep their feature expressivity in deep layers. [40] used a skip connection method that combined with node representations from different neighborhood ranges to preserve the locality of the node representations. [21] derived a personalized propagation of neural predictions (PPNP) based on personalized Pagerank. Other similar works using residual connection method could also be seen in [25, 9, 3, 28]. More recently, a series of latest works [46, 47, 26] explored the underlying reasons for performance degradation towards mitigation solutions, but the trainability of deep GNNs has not been theoretically investigated.

7 Conclusion and Discussion

In this work, we have characterized the asymptotic behavior of GNTK to measure the trainability of wide GCNs in the large depth. We prove that the trainability drops at an exponential rate due to the aggregation operation. Furthermore, we apply our theoretical framework to investigate the extent to which residual connection-resemble techniques could deepen GCNs. We demonstrate that these techniques can only slow down the decay speed, but are unable to solve the exponential decay problem in essence. To overcome the dropping trainability problem we further propose Critical DropEdge illuminated by our theoretical framework. The experimental results confirm that our method can address the trainability problems of deep GCNs. Future research directions include designing a critical node-centered method, so as to make better use of node information.

References

- [1] Zeyuan Allen-Zhu, Yuanzhi Li, and Zhao Song. A convergence theory for deep learning via over-parameterization. In *International Conference on Machine Learning*, pages 242–252. PMLR, 2019.
- [2] Sanjeev Arora, Simon S Du, Wei Hu, Zhiyuan Li, Russ R Salakhutdinov, and Ruosong Wang. On exact computation with an infinitely wide neural net. In *Advances in Neural Information Processing Systems*, pages 8141–8150, 2019.
- [3] Ming Chen, Zhewei Wei, Zengfeng Huang, Bolin Ding, and Yaliang Li. Simple and deep graph convolutional networks. In *International Conference on Machine Learning*, pages 1725–1735. PMLR, 2020.
- [4] Simon S Du, Kangcheng Hou, Russ R Salakhutdinov, Barnabas Poczos, Ruosong Wang, and Keyulu Xu. Graph neural tangent kernel: Fusing graph neural networks with graph kernels. In *Advances in Neural Information Processing Systems*, pages 5723–5733, 2019.
- [5] Simon S Du, Jason D Lee, Haochuan Li, Liwei Wang, and Xiyu Zhai. Gradient descent finds global minima of deep neural networks. *arXiv preprint arXiv:1811.03804*, 2018.
- [6] Paul Erdős and Alfréd Rényi. On the evolution of random graphs. In *The structure and dynamics of networks*, pages 38–82. Princeton University Press, 2011.
- [7] Ari Freedman. Convergence theorem for finite markov chains. *Proc. REU*, 2017.
- [8] Justin Gilmer, Samuel S Schoenholz, Patrick F Riley, Oriol Vinyals, and George E Dahl. Neural message passing for quantum chemistry. *arXiv preprint arXiv:1704.01212*, 2017.
- [9] Shunwang Gong, Mehdi Bahri, Michael M Bronstein, and Stefanos Zafeiriou. Geometrically principled connections in graph neural networks. In *Proceedings of the IEEE/CVF Conference on Computer Vision and Pattern Recognition*, pages 11415–11424, 2020.
- [10] Ingo Gühring, Mones Raslan, and Gitta Kutyniok. Expressivity of deep neural networks. *arXiv preprint arXiv:2007.04759*, 2020.
- [11] Will Hamilton, Zhitao Ying, and Jure Leskovec. Inductive representation learning on large graphs. In *Advances in neural information processing systems*, pages 1024–1034, 2017.
- [12] Soufiane Hayou, Arnaud Doucet, and Judith Rousseau. Mean-field behaviour of neural tangent kernel for deep neural networks. *arXiv preprint arXiv:1905.13654*, 2019.
- [13] Soufiane Hayou, Arnaud Doucet, and Judith Rousseau. On the impact of the activation function on deep neural networks training. *arXiv preprint arXiv:1902.06853*, 2019.
- [14] Jiri Hron, Yasaman Bahri, Jascha Sohl-Dickstein, and Roman Novak. Infinite attention: Nngp and ntk for deep attention networks. *arXiv preprint arXiv:2006.10540*, 2020.
- [15] Jiaoyang Huang and Horng-Tzer Yau. Dynamics of deep neural networks and neural tangent hierarchy. *arXiv preprint arXiv:1909.08156*, 2019.

- [16] Wei Huang, Weitao Du, and Richard Yi Da Xu. On the neural tangent kernel of deep networks with orthogonal initialization. *arXiv preprint arXiv:2004.05867*, 2020.
- [17] Wei Huang, Pengcheng Hou, Junfeng Wang, Robert M Ziff, and Youjin Deng. Critical percolation clusters in seven dimensions and on a complete graph. *Physical Review E*, 97(2):022107, 2018.
- [18] Arthur Jacot, Franck Gabriel, and Clément Hongler. Neural tangent kernel: Convergence and generalization in neural networks. In *Advances in neural information processing systems*, pages 8571–8580, 2018.
- [19] Thomas N Kipf and Max Welling. Semi-supervised classification with graph convolutional networks. *arXiv preprint arXiv:1609.02907*, 2016.
- [20] Thomas N Kipf and Max Welling. Variational graph auto-encoders. *arXiv preprint arXiv:1611.07308*, 2016.
- [21] Johannes Klicpera, Aleksandar Bojchevski, and Stephan Günnemann. Predict then propagate: Graph neural networks meet personalized pagerank. *arXiv preprint arXiv:1810.05997*, 2018.
- [22] Jaehoon Lee, Yasaman Bahri, Roman Novak, Samuel S Schoenholz, Jeffrey Pennington, and Jascha Sohl-Dickstein. Deep neural networks as Gaussian processes. *arXiv preprint arXiv:1711.00165*, 2017.
- [23] Jaehoon Lee, Lechao Xiao, Samuel Schoenholz, Yasaman Bahri, Roman Novak, Jascha Sohl-Dickstein, and Jeffrey Pennington. Wide neural networks of any depth evolve as linear models under gradient descent. In *Advances in neural information processing systems*, pages 8570–8581, 2019.
- [24] Junhyun Lee, Inyeop Lee, and Jaewoo Kang. Self-attention graph pooling. *arXiv preprint arXiv:1904.08082*, 2019.
- [25] Guohao Li, Matthias Muller, Ali Thabet, and Bernard Ghanem. Deepgcns: Can gcns go as deep as cnns? In *Proceedings of the IEEE/CVF International Conference on Computer Vision*, pages 9267–9276, 2019.
- [26] Guohao Li, Chenxin Xiong, Ali Thabet, and Bernard Ghanem. Deepergcn: All you need to train deeper gcns. *arXiv preprint arXiv:2006.07739*, 2020.
- [27] Qimai Li, Zhichao Han, and Xiao-Ming Wu. Deeper insights into graph convolutional networks for semi-supervised learning. *arXiv preprint arXiv:1801.07606*, 2018.
- [28] Meng Liu, Hongyang Gao, and Shuiwang Ji. Towards deeper graph neural networks. In *Proceedings of the 26th ACM SIGKDD International Conference on Knowledge Discovery & Data Mining*, pages 338–348, 2020.
- [29] Alexander G de G Matthews, Mark Rowland, Jiri Hron, Richard E Turner, and Zoubin Ghahramani. Gaussian process behaviour in wide deep neural networks. *arXiv preprint arXiv:1804.11271*, 2018.
- [30] Radford M Neal. Priors for infinite networks. In *Bayesian Learning for Neural Networks*, pages 29–53. Springer, 1996.
- [31] Kenta Oono and Taiji Suzuki. Graph neural networks exponentially lose expressive power for node classification. *arXiv preprint arXiv:1905.10947*, 2019.
- [32] Ben Poole, Subhaneil Lahiri, Maithra Raghu, Jascha Sohl-Dickstein, and Surya Ganguli. Exponential expressivity in deep neural networks through transient chaos. In *Advances in neural information processing systems*, pages 3360–3368, 2016.
- [33] Yu Rong, Wenbing Huang, Tingyang Xu, and Junzhou Huang. Dropedge: Towards deep graph convolutional networks on node classification. In *International Conference on Learning Representations*, 2019.

- [34] Ryan A. Rossi and Nesreen K. Ahmed. The network data repository with interactive graph analytics and visualization. In *AAAI*, 2015.
- [35] Samuel S Schoenholz, Justin Gilmer, Surya Ganguli, and Jascha Sohl-Dickstein. Deep information propagation. *arXiv preprint arXiv:1611.01232*, 2016.
- [36] Dietrich Stauffer and Ammon Aharony. *Introduction to percolation theory*. CRC press, 2018.
- [37] Petar Veličković, Guillem Cucurull, Arantxa Casanova, Adriana Romero, Pietro Lio, and Yoshua Bengio. Graph attention networks. *arXiv preprint arXiv:1710.10903*, 2017.
- [38] Lechao Xiao, Jeffrey Pennington, and Samuel S Schoenholz. Disentangling trainability and generalization in deep learning. *arXiv preprint arXiv:1912.13053*, 2019.
- [39] Keyulu Xu, Weihua Hu, Jure Leskovec, and Stefanie Jegelka. How powerful are graph neural networks? *arXiv preprint arXiv:1810.00826*, 2018.
- [40] Keyulu Xu, Chengtao Li, Yonglong Tian, Tomohiro Sonobe, Ken-ichi Kawarabayashi, and Stefanie Jegelka. Representation learning on graphs with jumping knowledge networks. *arXiv preprint arXiv:1806.03536*, 2018.
- [41] Keyulu Xu, Jingling Li, Mozhi Zhang, Simon S Du, Ken-ichi Kawarabayashi, and Stefanie Jegelka. How neural networks extrapolate: From feedforward to graph neural networks. *arXiv preprint arXiv:2009.11848*, 2020.
- [42] Ge Yang and Samuel Schoenholz. Mean field residual networks: On the edge of chaos. In *Advances in neural information processing systems*, pages 7103–7114, 2017.
- [43] Greg Yang. Scaling limits of wide neural networks with weight sharing: Gaussian process behavior, gradient independence, and neural tangent kernel derivation. *arXiv preprint arXiv:1902.04760*, 2019.
- [44] Greg Yang. Tensor programs ii: Neural tangent kernel for any architecture. *arXiv preprint arXiv:2006.14548*, 2020.
- [45] Hao Yuan and S. Ji. Structpool: Structured graph pooling via conditional random fields. In *ICLR*, 2020.
- [46] Hanqing Zeng, Muhan Zhang, Yinglong Xia, Ajitesh Srivastava, Rajgopal Kannan, Viktor Prasanna, Long Jin, Andrey Malevich, and Ren Chen. Deep graph neural networks with shallow subgraph samplers. *ICLR*, 2020.
- [47] Kaixiong Zhou, Xiao Huang, Yuening Li, Daochen Zha, Rui Chen, and Xia Hu. Towards deeper graph neural networks with differentiable group normalization. *arXiv preprint arXiv:2006.06972*, 2020.
- [48] Difan Zou, Yuan Cao, Dongruo Zhou, and Quanquan Gu. Stochastic gradient descent optimizes over-parameterized deep relu networks. arxiv e-prints, art. *arXiv preprint arXiv:1811.08888*, 2018.

A APPENDIX: A General GCN considered in this work

GCNs iteratively update node features through aggregating and transforming the representation of their neighbors. Figure 3 illustrates an overview of the information propagation in a general GCN.

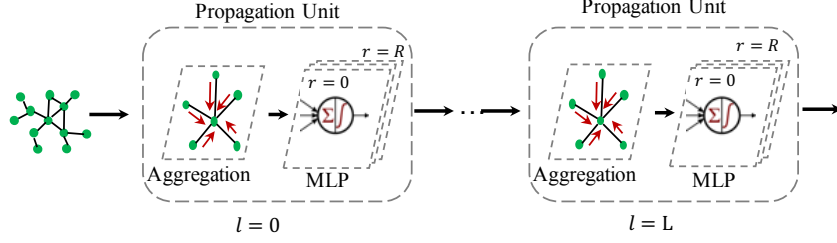


Figure 3: Overview of the information propagation in a general GCN.

B APPENDIX: Proofs for Theorem 1

B.1 Convergence of Aggregation GNTK

In theorem 1 we demonstrate that the matrix $\mathcal{A}(G)$ is a transition matrix, we first prove this proposition. To this end, we block the non-linear transformation by setting $R = 0$. Then and the propagation of GNTK can be expressed as,

$$\Theta^{(l)}(u, u') = \frac{1}{|\mathcal{N}(u)| + 1} \frac{1}{|\mathcal{N}(u')| + 1} \sum_{v \in \mathcal{N}(u) \cup u} \sum_{v' \in \mathcal{N}(u') \cup u'} \Theta^{(l-1)}(v, v') \quad (14)$$

In order to facilitate calculation, we rewrite Equation (14) as the following format,

$$\vec{\Theta}^{(l)}(G) = \mathcal{A}(G) \vec{\Theta}^{(l-1)}(G) \quad (15)$$

where $\vec{\Theta}^{(l)}(G) \in \mathbb{R}^{n^2 \times 1}$ is the result of being vectorized, and the matrix $\mathcal{A}(G) \in \mathbb{R}^{n^2 \times n^2}$ is a square matrix. We show the key result that $\mathcal{A}(G)$ is a probability transition matrix, and the limiting behavior of $\Theta^{(l)}(\mathcal{V}, \mathcal{V})$ in the following lemma,

Lemma 1 (Convergence of Aggregation). *Assume $R = 0$, then*

$$\lim_{l \rightarrow \infty} \Theta^{(l)}(u, u') = \bar{\pi}(G)^T \vec{\Theta}^{(0)}(G)$$

where $\bar{\pi}(G) \in \mathbb{R}^{n^2 \times 1}$, satisfying $\mathcal{A}(G) \bar{\pi}(G) = \bar{\pi}(G)$.

Proof. When $R = 0$, Equation (14) reduces to,

$$\Theta^{(l)}(u, u') = \frac{1}{|\mathcal{N}(u)| + 1} \frac{1}{|\mathcal{N}(u')| + 1} \sum_{v \in \mathcal{N}(u) \cup u} \sum_{v' \in \mathcal{N}(u') \cup u'} \Theta^{(l-1)}(v, v')$$

In order to facilitate calculation, we rewrite the above equation in the format of matrix,

$$\vec{\Theta}^{(l)}(G) = \mathcal{A}^{(l)}(G) \vec{\Theta}^{(l-1)}(G)$$

where $\vec{\Theta}^{(l)}(G) \in \mathbb{R}^{n^2 \times 1}$, is the result of being vectorized. Thus the matrix operation $\mathcal{A}^{(l)}(G) \in \mathbb{R}^{n^2 \times n^2}$. It is obvious that,

$$\mathcal{A}^{(L)}(G) = \mathcal{A}^{(L-1)}(G) = \dots = \mathcal{A}^{(l)}(G) = \dots = \mathcal{A}^{(1)}(G)$$

This implies that the aggregate operation is the same for each layer. The next step is to prove $\mathcal{A}(G)$ is a stochastic matrix (transition matrix):

$$\sum_j \mathcal{A}(G)_{ij} = 1.$$

According to Equation (14), $\mathcal{A}(G)$ can be expressed as a Kronecker product of two matrix,

$$\mathcal{A}(G) = [\mathcal{B}(G)\mathcal{C}(G)] \otimes [\mathcal{B}(G)\mathcal{C}(G)]$$

where $\mathcal{B}(G), \mathcal{C}(G) \in \mathbb{R}^{n \times n}$. We then analyse the two matrices separately:

(1) $\mathcal{B}(G)$ is a diagonal matrix, which corresponds to the factor $\frac{1}{\mathcal{N}(u)+1}$.

$$\mathcal{B}(G) = \begin{pmatrix} \frac{1}{\mathcal{N}(u_1)+1} & & \\ & \ddots & \\ & & \frac{1}{\mathcal{N}(u_n)+1} \end{pmatrix}$$

(2) The element of matrix $\mathcal{C}(G)$ is determined by whether there is a edge between two vertexes,

$$\mathcal{C}(G)_{ij} = \tilde{\delta}_{ij}$$

where $\tilde{\delta}_{ij} = 1$ if $i = j$ or there is edge between vertex i and j , else $\tilde{\delta}_{ij} = 0$.

We then use the property of matrix \mathcal{B} and \mathcal{C} before Kronecker product,

$$\sum_j [\mathcal{B}(G)\mathcal{C}(G)]_{ij} = \frac{1}{\mathcal{N}(u_i)+1} \sum_j \tilde{\delta}_{ij} = \frac{1}{\mathcal{N}(u_i)+1} (\mathcal{N}(u_i)+1) = 1$$

According to the definition of Kronecker product, we have,

$$\sum_j \mathcal{A}^{(l)}(G)_{ij} = \sum_b \sum_d [\mathcal{B}(G)\mathcal{C}(G)]_{ab} [\mathcal{B}(G)\mathcal{C}(G)]_{cd} = 1$$

where $i = a + (c-1)n$, and $j = b + (d-1)n$.

So far, we have proved that $\mathcal{A}(G)$ is a stochastic matrix. According to the Perron-Frobenius Theory, a stationary probability vector $\vec{\pi}(G) \in \mathbb{R}^{n^2 \times 1}$ is defined as a distribution, that does not change under application of the transition matrix; that is, it is defined as a probability distribution which is also a eigenvector of the probability matrix, associated with eigenvalue 1:

$$\mathcal{A}(G)\vec{\pi}(G) = \vec{\pi}(G)$$

Note that the spectral radius of every stochastic matrix is at most 1 by Gershgorin circle theorem. Thus the convergence rate is governed by the second largest eigenvalue.

Since $\lim_{l \rightarrow \infty} \mathcal{A}_{ij}^{(l)}(G) = \vec{\pi}_j(G)$, we have,

$$\lim_{l \rightarrow \infty} \vec{\Theta}^{(l)}(G) = \lim_{l \rightarrow \infty} \mathcal{A}^l(G)\vec{\Theta}^{(0)}(G) = \Pi(G)\vec{\Theta}^{(0)}(G)$$

where $\Pi(G) = \begin{pmatrix} \vec{\pi}(G)^T \\ \vec{\pi}(G)^T \\ \vdots \\ \vec{\pi}(G)^T \end{pmatrix}$ is the $n^2 \times n^2$ matrix all of whose rows are the stationary distribution.

Then, we can see that every element in $\vec{\Theta}^{(l)}(G)$ converges exponentially to an identical value, depending on the stationary distribution and initial state,

$$\lim_{l \rightarrow \infty} \Theta^{(l)}(u, u') = \vec{\pi}(G)^T \vec{\Theta}^{(0)}(G)$$

□

Remark 1. This lemma can be extended to the multi-graph setting, where matrix $\mathcal{A}(G, G') \in \mathbb{R}^{nn' \times nn'}$ with respect to a pair of graphs G, G' is a transition matrix as well, and n' is the number of vertexes in graph G' .

B.2 Convergence of MLP GPK

Before we prove Theorem 1, we introduce the result for the Gaussian Process kernel $\Sigma_{(r)}^{(l)}(G)$ of a pure MLP. By doing so, we consider a network with only non-linear transformation, which is known as a pure MLP. This leads to $\Sigma_{(r)}^{(l)}(u, u') = \Sigma_{(r)}(u, u')$, where we use subscript (r) to denote the layer index. And we rewrite the propagation function for GPK as follows,

$$\Sigma_{(r)}(u, u') = \sigma_w^2 \mathbb{E}_{z_1, z_2 \sim \mathcal{N}(0, \tilde{\Sigma}_{(r-1)})} [\phi(z_1)\phi(z_2)] + \sigma_b^2 \quad (16)$$

and the variance $\tilde{\Sigma}_{(r)} \in \mathbb{R}^{2 \times 2}$ is,

$$\tilde{\Sigma}_{(r)} = \begin{pmatrix} \Sigma_{(r)}(u, u) & \Sigma_{(r)}(u, u') \\ \Sigma_{(r)}(u', u) & \Sigma_{(r)}(u', u') \end{pmatrix} \quad (17)$$

The large depth behavior has been well studied in [13], and we introduce the result when the *edge of chaos* is realized. In particular, we set the value of hyper-parameters to satisfy,

$$\sigma_w^2 \int \mathcal{D}_z [\phi'(\sqrt{q^*}z)]^2 = 1 \quad (18)$$

where q^* is the fixed point of diagonal elements in the covariance matrix, and $\int \mathcal{D}z = \frac{1}{\sqrt{2\pi}} \int dz e^{-\frac{1}{2}z^2}$ is the measure for a normal distribution. For the ReLU activation, Equation (18) requires $\sigma_w^2 = 2$ and $\sigma_b^2 = 0$.

The key idea is to study the asymptotic behavior of the normalized correlation defined as,

$$C_r(u, u') \equiv \frac{\Sigma_{(r)}(u, u')}{\sqrt{\Sigma_{(r)}(u, u) \Sigma_{(r)}(u', u')}}. \quad (19)$$

Lemma 2 (Proposition 1 and 3 in [13]). *Assume a network without aggregation, i.e., $L = 0$, with a Lipschitz nonlinearity ϕ , then,*

- $\phi(x) = (x)_+$, $1 - C_r(u, u') \sim \frac{9\pi^2}{2r^2}$ as $r \rightarrow \infty$
- $\phi(x) = \tanh(x)$, $1 - C_r(u, u') \sim \frac{\beta}{r}$ as $r \rightarrow \infty$ where $\beta = \frac{2 \int_{\mathcal{D}_z} [\phi'(\sqrt{q^*}z)]^2}{q \int_{\mathcal{D}_z} [\phi''(\sqrt{q^*}z)]^2}$.

Proof. We first decompose the integral calculation in the Equation (16) into two parts, one is diagonal element and the other is non-diagonal element:

$$\begin{aligned} \Sigma_{(r)}(u, u) &= \sigma_w^2 \int_{\mathcal{D}z} \phi^2(\sqrt{\Sigma_{(r-1)}(u, u)}z) + \sigma_b^2 \\ \Sigma_{(r)}(u, u') &= \sigma_w^2 \int_{\mathcal{D}z_1 \mathcal{D}z_2} \phi(u_1)\phi(u_2) + \sigma_b^2 \end{aligned}$$

where $u_1 = \sqrt{\Sigma_{(r-1)}(u, u)}z_1$, and $u_2 = \sqrt{\Sigma_{(r-1)}(u', u')} \left(C_{r-1}(u, u')z_1 + \sqrt{1 - C_{r-1}^2(u, u')}z_2 \right)$, with $C_{r-1}(u, u') = \Sigma_{(r-1)}(u, u') / \sqrt{\Sigma_{(r-1)}(u, u) \Sigma_{(r-1)}(u', u')}$.

For simplicity, we define $q_r(u) = \Sigma_{(r)}(u, u)$, $q_r(u') = \Sigma_{(r)}(u', u')$. We then process the proof by dividing the activation $\phi(x)$ into two classes, namely, ReLU and Tanh.

ReLU activation, $\phi(x) = \max\{0, x\}$. The recursive equation (16) for $q_r(u)$ reduces to,

$$q_r(u) = \frac{\sigma_w^2}{2} q_{r-1}(u) + \sigma_b^2$$

The edge of chaos condition $\sigma_w^2 \int \mathcal{D}_z [\phi'(\sqrt{q^*}z)]^2 = 1$ requires $\sigma_w^2 = 2$ and $\sigma_b^2 = 0$ for ReLU activation, which leads to,

$$\lim_{r \rightarrow \infty} q_r(u) = q_0(u) \equiv q(u)$$

Then the second integration for $C_r(u, u')$ becomes,

$$C_r(u, u') = \frac{\sigma_w^2 \int_{\mathcal{D}z_1 \mathcal{D}z_2} \phi(\sqrt{q_{r-1}(u)}z_1) \phi(\sqrt{q_{r-1}(u')} (C_{r-1}(u, u')z_1 + \sqrt{1 - C_{r-1}^2(u, u')}z_2)) + \sigma_b^2}{q_{r-1}(u)}$$

To investigate the propagation of $C_r(u, u')$, we set $q_r(u) = q_r(u') = q$, and define,

$$f(x) = \frac{\sigma_w^2 \int_{\mathcal{D}z_1 \mathcal{D}z_2} \phi(\sqrt{q}z_1) \phi(\sqrt{q}(xz_1 + \sqrt{1 - x^2}z_2)) + \sigma_b^2}{q}$$

Let $x \in [0, 1]$, the derivative of $f(x)$ satisfies,

$$f'(x) = 2 \int_{\mathcal{D}_{z_1} \mathcal{D}_{z_2}} 1_{z_1 > 0} 1_{xz_1 + \sqrt{1-x^2}z_2 > 0}$$

This can be seen from a simple derivation,

$$\begin{aligned} f'(x) &= \int_{\mathcal{D}_{z_1}} \int_{\mathcal{D}_{z_2}} \phi(z_1) \phi'(xz_1 + \sqrt{1-x^2}z_2) (z_1 - \frac{x}{\sqrt{1-x^2}}z_2) \\ &= \int_{\mathcal{D}_{z_1}} \int_{\mathcal{D}_{z_2}} \phi(z_1) \phi'(xz_1 + \sqrt{1-x^2}z_2) (z_1) - \int_{\mathcal{D}_{z_1}} \int_{\mathcal{D}_{z_2}} \phi(z_1) \phi'(xz_1 + \sqrt{1-x^2}z_2) (\frac{x}{\sqrt{1-x^2}}z_2) \end{aligned}$$

Using an identity for Gaussian integration $\int_{\mathcal{D}_z} zg(z) = \int_{\mathcal{D}_z} g'(z)$ yields,

$$\begin{aligned} f'(x) &= \int_{\mathcal{D}_{z_1}} \int_{\mathcal{D}_{z_2}} [\phi'(z_1) \phi'(xz_1 + \sqrt{1-x^2}z_2) + \phi(z_1) \phi''(xz_1 + \sqrt{1-x^2}z_2) - \phi(z_1) \phi''(xz_1 + \sqrt{1-x^2}z_2)] \\ &= \int_{\mathcal{D}_{z_1}} \int_{\mathcal{D}_{z_2}} \phi'(z_1) \phi'(xz_1 + \sqrt{1-x^2}z_2) \end{aligned}$$

Then the second derivative of $f(x)$ becomes, $f''(x) = \frac{1}{\pi\sqrt{1-x^2}}$. So using the equation above and the condition $f'(0) = \frac{1}{2}$, we can get another formation of the derivative of $f(x)$,

$$f'(x) = \frac{1}{\pi} \arcsin(x) + \frac{1}{2}$$

Because $\int \arcsin = x \arcsin + \sqrt{1-x^2}$ and $f(1) = 1$, then for $x \in [0, 1]$,

$$f(x) = \frac{2x \arcsin(x) + 2\sqrt{1-x^2} + x\pi}{2\pi}$$

Substituting $f(x) = C_r(u, u')$ and $x = C_{r-1}(u, u')$, into expression up here, we have,

$$C_r(u, u') = \frac{2C_{r-1}(u, u') \arcsin(C_{r-1}(u, u')) + 2\sqrt{1-C_{r-1}^2(u, u')} + C_{r-1}(u, u')\pi}{2\pi}$$

Now we study the behavior of $C_r(u, u')$ as r tends to infinity. Using Taylor expansion, we have,

$$f(x)|_{x \rightarrow 1^-} = x + \frac{2\sqrt{2}}{3\pi}(1-x)^{3/2} + O((1-x)^{5/2})$$

By induction analysis, the sequence $C_r(u, u')$ is increasing to the fixed point 1. Besides, we can replace x with $C_r(u, u')$,

$$C_{r+1}(u, u') = C_r(u, u') + \frac{2\sqrt{2}}{3\pi}(1-C_r(u, u'))^{3/2} + O((1-C_r(u, u'))^{5/2})$$

Let $\gamma_r = 1 - C_r(u, u')$, then we have,

$$\gamma_{r+1} = \gamma_r - \frac{2\sqrt{2}}{3\pi}\gamma_r^{3/2} + O(\gamma_r^{5/2})$$

so that,

$$\gamma_{r+1}^{-1/2} = \gamma_r^{-1/2} (1 - \frac{2\sqrt{2}}{3\pi}\gamma_r^{1/2} + O(\gamma_r^{3/2}))^{-1/2} = \gamma_r^{-1/2} + \frac{\sqrt{2}}{3\pi} + O(\gamma_r)$$

As r tends to infinity, we have,

$$\gamma_{r+1}^{-1/2} - \gamma_r^{-1/2} \sim \frac{\sqrt{2}}{3\pi}$$

It means,

$$\gamma_r^{-1/2} \sim \frac{\sqrt{2}}{3\pi}r$$

Therefore, we have,

$$1 - C_r(u, u') \sim \frac{9\pi^2}{2r^2}$$

Tanh activation, $\phi(x) = \tanh(x)$. For the argument of fixed point, we ask readers to refer to [13]. Here we only discuss the convergence rate of GPK, which means we directly assume that $f(x)$ tends to be 1 as the depth tends to be infinity $\lim_{r \rightarrow \infty} C_r(u, u') = 1$. For the function $f(x)$, a Taylor expansion near 1 yields,

$$f(x) = 1 + (x - 1)f'(1) + \frac{(x - 1)^2}{2}f''(1) + O((x - 1)^{5/2})$$

where $f'(1) = \sigma_w^2 \int_{\mathcal{D}_z} [\phi'(\sqrt{q}z)^2]$, and $f''(1) = \sigma_w^2 q \int_{\mathcal{D}_z} [\phi''(\sqrt{q}z)^2]$. Denote $\gamma_r = 1 - C_r(u, u')$, then we have,

$$\gamma_{r+1} = \gamma_r - \frac{\gamma_r^2}{\beta} + O(\gamma_r^{5/2})$$

where $\beta = \frac{2 \int_{\mathcal{D}_z} [\phi'(\sqrt{q^*}z)^2]}{q \int_{\mathcal{D}_z} [\phi''(\sqrt{q^*}z)^2]}$. Therefore,

$$\gamma_{r+1}^{-1} = \gamma_r^{-1} \left(1 - \frac{\gamma_r}{\beta} + O(\gamma_r^{3/2})\right) = \gamma_r^{-1} + \frac{1}{\beta} + O(\gamma_r^{1/2}).$$

Thus, we have,

$$1 - C_{(r)}(u, u') \sim \frac{\beta}{r} \text{ as } r \rightarrow \infty$$

□

Lemma 2 shows the covariance matrix converges to a constant matrix at a polynomial rate of $1/r^2$ for ReLU and of $1/r$ for tanh activation on the edge of chaos. This implies that a network without aggregation could retain its expressivity at a large depth. However, for general case, due to the aggregation, the rate of convergence will change from polynomial to exponential. This will make the trainability of the deep graph network problematic, which will be shown in the following section.

B.3 Convergence of GPK for GCNs

Then we formally characterize the convergence of Gaussian Process kernel $\Sigma_{(r)}^{(l)}(u, u')$ of a GCN in the infinite-width limit:

Lemma 3. *If $\mathcal{A}(G)$ is irreducible and aperiodic, with a stationary distribution vector $\vec{\pi}(G)$, then there exist constants $0 < \alpha < 1$ and $C > 0$, and constant vector $\vec{v} \in \mathbb{R}^{n^2 \times 1}$ depending on the number of MLP iterations R , such that*

$$|\Sigma_{(r)}^{(l)}(u, u') - \vec{\pi}(G)^T \vec{v}| \leq C\alpha^l$$

Proof. We prove the result by induction method. For $l = 0$, according to the Cauchy-Buniakowsky-Schwarz Inequality

$$\Sigma_{(0)}^{(0)}(u, u') = h_u^{(0)} h_{u'}^{(0)} \leq \|h_u^{(0)}\|_2 \|h_{u'}^{(0)}\|_2 = 1$$

Thus there is a constant C , depending on $G(V, E)$, and the number of MLP operation R , over feature initialization, such that,

$$|\Sigma_{(0)}^{(0)}(u, u') - \vec{\pi}(G)^T \vec{v}| < C$$

Assume the result is valid for $\Sigma_{(r)}^{(l)}(u, u')$, then we have,

$$|\Sigma_{(r)}^{(l)}(u, u') - \vec{\pi}(G)^T \vec{v}| \leq C_0 \alpha^l$$

where C_0 is a constant satisfying $0 < C_0 < C$. Now we consider the distance between $\Sigma_{(r)}^{(l+1)}(u, u')$ and $C\alpha^{l+1}$. To compute this, we need to divide the propagation from l layer to $l + 1$ layer into three steps:

1. $\Sigma_{(r)}^{(l)} \rightarrow \Sigma_{(r+1)}^{(l)} \rightarrow \dots \rightarrow \Sigma_{(R)}^{(l)}$

2. $\Sigma_{(R)}^{(l)} \rightarrow \Sigma_{(0)}^{(l+1)}$
3. $\Sigma_{(0)}^{(l+1)} \rightarrow \Sigma_{(1)}^{(l+1)} \rightarrow \dots \rightarrow \Sigma_{(r)}^{(l+1)}$.

It is not hard to find that steps 1,3 correspond to non-linear transformation while step 2 corresponds with aggregation operation, we then characterize them one by one,

MLP Propagation The assumption $|\Sigma_{(r)}^{(l)}(u, u') - \bar{\pi}(G)^T \bar{v}| \leq C_0 \alpha^l$ implicitly implies that $C_r(u, u')$ is close to one. Because $C_r(u, u') = \frac{\Sigma_{(r)}^{(l)}(u, u')}{\sqrt{\Sigma_{(r)}^{(l)}(u, u) \Sigma_{(r)}^{(l)}(u', u')}}}$, then,

$$\frac{\bar{\pi}(G)^T \bar{v} - C_0 \alpha^l}{\bar{\pi}(G)^T \bar{v} + C_0 \alpha^l} \leq C_r(u, u') \leq \frac{\bar{\pi}(G)^T \bar{v} + C_0 \alpha^l}{\bar{\pi}(G)^T \bar{v} - C_0 \alpha^l}$$

Because $C_0 \alpha^l \ll \bar{\pi}(G)^T \bar{v}$, we have $C_r(u, u') = 1 + O(\alpha^l)$. Recall the property of MLP propagation function $f(x)$ for $x = C_r(u, u')$, when $C_r(u, u')$ is close to 1:

$$f(x)|_{x \rightarrow 1-} = x + \frac{2\sqrt{2}}{3\pi}(1-x)^{3/2} + O((1-x)^{5/2})$$

This implies,

$$|C_{(r+1)}(u, u') - C_{(r)}(u, u')| = \frac{2\sqrt{2}}{3\pi}(1 - C_{(r)}(u, u'))^{\frac{3}{2}} + O(1 - C_{(r)}(u, u'))^{\frac{5}{2}} = O(\alpha^{\frac{3}{2}l})$$

With this result, we can further obtain,

$$\begin{aligned} |\Sigma_{(r+1)}^{(l)}(u, u') - \bar{\pi}(G)^T \bar{v}| &= |\Sigma_{(r+1)}^{(l)}(u, u') - \Sigma_{(r)}^{(l)}(u, u') + \Sigma_{(r)}^{(l)}(u, u') - \bar{\pi}(G)^T \bar{v}| \\ &\leq |\Sigma_{(r+1)}^{(l)}(u, u') - \Sigma_{(r)}^{(l)}(u, u')| + |\Sigma_{(r)}^{(l)}(u, u') - \bar{\pi}(G)^T \bar{v}| \\ &= |C_{(r+1)}^{(l)}(u, u') - C_{(r)}^{(l)}(u, u')| \sqrt{\Sigma_{(r)}^{(l)}(u, u) \Sigma_{(r)}^{(l)}(u', u')} + |\Sigma_{(r)}^{(l)}(u, u') - \bar{\pi}(G)^T \bar{v}| \\ &= C_1 \alpha^{\frac{3}{2}l} + C_0 \alpha^l \leq (C_0 + C_1) \alpha^l. \end{aligned}$$

where C_1 is a positive constant. Repeat the proof process, we have a relation for $\Sigma_{(R)}^{(l)}(u, u')$ at the last step of 1,

$$|\Sigma_{(R)}^{(l)}(u, u') - \bar{\pi}(G)^T \bar{v}| \leq (C_0 + (R-r)C_1) \alpha^l. \quad (20)$$

Aggregation Propagation We go through an aggregation operation $\mathcal{A}(G)$. In this case, we use a formation of matrix, and take Equation (20) into aggregation function, yields the result as follows,

$$\bar{\Sigma}_{(0)}^{(l+1)}(G) = \mathcal{A}(G) \bar{\Sigma}_{(R)}^{(l)}(G) = \mathcal{A}(G) (\Pi(G) \bar{v} + \bar{O}(\alpha^l))$$

where $\bar{O}(\alpha^l) \in \mathbb{R}^{n^2 \times 1}$ denotes a vector in which every element is bounded by α^l .

According to the theorem 4.9 in [7], we have $\mathcal{A}^l \Pi(G) \bar{v} = \Pi(G) \bar{v}$ as $l \rightarrow \infty$. When l is finite, the error is of exponential decay. Here we use $0 < \alpha < 1$ to denote the corresponding base number. Therefore,

$$|\Sigma_{(0)}^{(l+1)}(u, u') - \bar{\pi}(G)^T \bar{v}| \leq (C_0 + (R-r)C_1) \alpha^{l+1}.$$

Finally, Repeat the result in step 1, we have,

$$|\Sigma_{(r)}^{(l+1)}(u, u') - \bar{\pi}(G)^T \bar{v}| \leq (C_0 + RC_1) \alpha^{l+1} = C \alpha^{l+1}.$$

□

Remark 2. In the proof, there is a RC_1 term in each propagation of $l \rightarrow l+1$, which may lead to explosion when l tends to infinity. Basically, this problem can be solved by a careful analysis, because the constant C_1 is associated with $O(\alpha^{\frac{3}{2}l})$ which is a smaller order compared to $O(\alpha^l)$.

B.4 Convergence of the GNTK

Finally, we arrive at our main theorem:

Theorem 1 (Convergence Rate of the GNTK). *If $\mathcal{A}(G)$ is irreducible and aperiodic, with a stationary distribution vector $\bar{\pi}(G)$, then there exist constants $0 < \alpha < 1$ and $C > 0$, and constant vector $\bar{v}, \bar{v}' \in \mathbb{R}^{n^2 \times 1}$ depending on the number of MLP iterations R , such that*

$$|\Theta_{(r)}^{(l)}(u, u') - \bar{\pi}(G)^T (Rl\bar{v} + \bar{v}')| \leq C\alpha^l$$

Proof. This proof has the same strategy to that of Lemma 3. The first step is to understand the Equation (9) in the large-depth limit.

$$\Theta_{(r)}^{(l)}(u, u') = \Theta_{(r-1)}^{(l)}(u, u') \dot{\Sigma}_{(r)}^{(l)}(u, u') + \Sigma_{(r)}^{(l)}(u, u')$$

According to the result of Lemma 3, we have already known,

$$\Sigma_{(r)}^{(l)}(u, u') = \bar{\pi}(G)^T \bar{v} + O(\alpha^l)$$

To proceed the proof, we need to work out the behavior of $\dot{\Sigma}_{(r)}^{(l)}(u, u')$ in the large depth.

ReLU activation, $\phi(x) = \max\{0, x\}$. Recall that we define $C_{r+1} = f(C_r)$, and we have,

$$f'(x) = \frac{1}{\pi} \arcsin(x) + \frac{1}{2}$$

Then, at the edge of chaos,

$$\begin{aligned} \dot{\Sigma}_{(r)}^{(l)}(u, u') &= f'(C_r(u, u')) = \frac{1}{\pi} \arcsin(C_r(u, u')) + \frac{1}{2} \\ &= 1 - \frac{2}{\pi} (1 - C_r(u, u'))^{1/2} + O(1 - C_r(u, u'))^{3/2} = 1 + O(\alpha^{l/2}) \end{aligned}$$

Tanh activation, $\phi(x) = \tanh(x)$. We have

$$f'(x) = 1 - (x - 1)f''(1) + O((x - 1)^2)$$

At the edge of chaos,

$$\dot{\Sigma}_{(r)}^{(l)}(u, u') = 1 + O(\alpha^l)$$

Now we prove the result by induction method. For $l = 0$, we directly have,

$$\Theta_{(0)}^{(0)}(u, u') = \Sigma_{(0)}^{(0)}(u, u') \leq \|h_u^{(0)}\|_2 \|h_{u'}^{(0)}\|_2 = 1$$

Thus there is a constant C , depending on $G(V, E)$, and the number of MLP operation R , over feature initialization,

$$|\Theta_{(0)}^{(0)}(u, u') - \bar{\pi}(G)^T \bar{v}'| < C$$

Assume the result is valid for $\Theta_{(r)}^{(l)}(u, u')$, then we have,

$$|\Theta_{(r)}^{(l)}(u, u') - \bar{\pi}(G)^T (Rl\bar{v} + \bar{v}')| \leq C\alpha^l$$

Now we consider the distance between $\Theta_{(r)}^{(l+1)}(u, u')$ and $\bar{\pi}(G)^T (R(l+1)\bar{v} + \bar{v}')$. To prove this, we need to divide the propagation from l layer to $l+1$ layer into three steps:

1. $\Theta_{(r)}^{(l)} \rightarrow \Theta_{(r+1)}^{(l)} \rightarrow \dots \rightarrow \Theta_{(R)}^{(l)}$
2. $\Theta_{(R)}^{(l)} \rightarrow \Theta_{(0)}^{(l+1)}$

$$3. \Theta_{(0)}^{(l+1)} \rightarrow \Theta_{(1)}^{(l+1)} \rightarrow \dots \rightarrow \Theta_{(r)}^{(l+1)}.$$

For step 1, we have,

$$\begin{aligned} & |\Theta_{(r+1)}^{(l)}(u, u') - \bar{\pi}(G)^T((lR+1)\vec{v} + \vec{v}')| \\ &= |\Sigma_{(r+1)}^{(l)}(u, u') + \dot{\Sigma}_{(r+1)}^{(l)}(u, u')\Theta_{(r)}^{(l)}(u, u') - \bar{\pi}(G)^T((lR+1)\vec{v} + \vec{v}')| \\ &= |\bar{\pi}(G)^T\vec{v}(1 + O(\alpha^l)) + (1 + O(\alpha^{l/2}))\Theta_{(r)}^{(l)}(u, u') - \bar{\pi}(G)^T((lR+1)\vec{v} + \vec{v}')| \leq C\alpha^l \end{aligned}$$

Repeat the process, we have a relation for $\Theta_{(R)}^{(l)}(u, u')$ at the last transformation in step 1,

$$|\Theta_{(R)}^{(l)}(u, u') - \bar{\pi}(G)^T((lR+R-r)\vec{v} + \vec{v}')| \leq C\alpha^l.$$

Secondly, we go through an aggregation operation. Because it is a Markov chain step, we have,

$$|\Theta_{(0)}^{(l+1)}(u, u') - \bar{\pi}(G)^T((Rl+R-r)\vec{v} + \vec{v}')| \leq C\alpha^{l+1}.$$

Repeat the result in step 1, we finally have,

$$\begin{aligned} & |\Theta_{(r)}^{(l+1)}(u, u') - \bar{\pi}(G)^T((Rl+R)\vec{v} + \vec{v}')| \\ &= |\Theta_{(r)}^{(l+1)}(u, u') - \bar{\pi}(G)^T(R(l+1)\vec{v} + \vec{v}')| \leq C\alpha^{l+1}. \end{aligned}$$

□

Corollary 1 (Trainability of Ultra-Wide GCNs). *Consider a GCN of the form (6) and (7), with depth L , non-linear transformations number R , an MSE loss, and a Lipchitz activation $\phi(x)$, trained with gradient descent on a node classification task. Then the output function follows,*

$$f_t(\mathcal{V}) = e^{-\eta\Theta_{(R)}^{(L)}(\mathcal{V}, \mathcal{V})t} f_0(\mathcal{V}) + (I - e^{-\eta\Theta_{(R)}^{(L)}(\mathcal{V}, \mathcal{V})t})\mathcal{Y}$$

where \mathcal{Y} is the label with respect to node \mathcal{V} . Then, there exists a positive integer L_0 such that, $\Theta_{(R)}^{(L)}(\mathcal{V}, \mathcal{V})$ is singular when $L > L_0$. Moreover, there exist a constant $C > 0$ such that for all $t > 0$,

$$\|f_t(\mathcal{V}) - \mathcal{Y}\| > C$$

Proof. According to the result from [18], GNTK $\Theta_{(r)}^{(l)}(\mathcal{V}, \mathcal{V})$ converges to a deterministic kernel and remains constant during gradient descent in the infinite width limit. We omit proof procedure for this result, since it is now a standard conclusion in the NTK study.

Based on the conclusion above, [23] proved that the infinitely-wide neural network is equivalent to its linearized mode,

$$f_t^{\text{lin}}(\mathcal{V}) = f_0(\mathcal{V}) + \nabla_{\theta} f_0(\mathcal{V})|_{\theta=\theta_0} \omega_t$$

where $\omega_t = \theta_t - \theta_0$. We call it linearized model because only zero and first order term of Taylor expansion are kept. Since we know dynamics of gradient flow using this linearized function are governed by,

$$\dot{\omega}_t = -\eta \nabla_{\theta} f_0(\mathcal{V})^T \nabla_{f_t^{\text{lin}}(\mathcal{V})} \mathcal{L}$$

$$\dot{f}_t^{\text{lin}}(\mathcal{V}) = -\eta \Theta_{(r)}^{(l)}(\mathcal{V}, \mathcal{V}) \nabla_{f_t^{\text{lin}}(\mathcal{V})} \mathcal{L}$$

where \mathcal{L} is an MSE loss, then the above equations have closed form solutions

$$f_t^{\text{lin}}(\mathcal{V}) = e^{-\eta\Theta_{(r)}^{(l)}(\mathcal{V}, \mathcal{V})t} f_0(\mathcal{V}) + (I - e^{-\eta\Theta_{(r)}^{(l)}(\mathcal{V}, \mathcal{V})t})\mathcal{Y}$$

Since Lee et al. [23] showed that $f_t^{\text{lin}}(\mathcal{V}) = f_t$ in the infinite width limit, thus we have,

$$f_t(\mathcal{V}) = e^{-\eta\Theta_{(r)}^{(l)}(\mathcal{V}, \mathcal{V})t} f_0(\mathcal{V}) + (I - e^{-\eta\Theta_{(r)}^{(l)}(\mathcal{V}, \mathcal{V})t})\mathcal{Y} \quad (21)$$

In theorem 1, we have shown $\Theta_{(r)}^{(l)}(\mathcal{V}, \mathcal{V})$ converges a constant matrix at an exponential rate. According to Equation (21), we know that,

$$\|f_t(\mathcal{V}) - \mathcal{Y}\| = \|e^{-\eta\Theta_{(r)}^{(l)}(\mathcal{V}, \mathcal{V})t}(f_0(\mathcal{V}) - \mathcal{Y})\|$$

According to Theorem 1, there exists a l_0 such that, for any $l > l_0$, the GNTK converges to a constant matrix,

$$\Theta_{(r)}^{(l)}(\mathcal{V}, \mathcal{V}) = \Theta(\mathcal{V}, \mathcal{V})$$

Then the GNTK $\Theta_{(r)}^{(l)}(\mathcal{V}, \mathcal{V})$ is singular. Let $\Theta_{(r)}^{(l)}(\mathcal{V}, \mathcal{V}) = Q^T D Q$ be the decomposition of the GNTK, where Q is an orthogonal matrix and D is a diagonal matrix. Because $\Theta_{(r)}^{(l)}(\mathcal{V}, \mathcal{V})$ is singular, D has at least one zero value $d_j = 0$, then

$$\|f_t(\mathcal{V}) - \mathcal{Y}\| = \|Q^T (f_t(\mathcal{V}) - \mathcal{Y}) Q\| \geq \| [Q^T (f_0(\mathcal{V}) - \mathcal{Y}) Q]_j \|$$

□

Remark 3. *In the proof we assume the loss is MSE. Nevertheless, the conclude regarding trainability can be applied to other common loss such as cross-entropy. For cross-entropy loss, even though we cannot write down an analytical expression for the solution, we prove the GNTK still governs the trainability and the law of GNTK is not affected by the loss. Thus the results for trainability hold on the cross-entropy case.*

C Convergence of Residual GNTK

C.1 Residual connection in aggregation

Theorem 2 (Convergence rate for residual connection in aggregation). *Consider a GNTK of the form (12) with non-linear transformation of the form (7). Then with a stationary vector $\tilde{\pi}(G)$ for $\tilde{A}(G)$, there exist constants $0 < \alpha < 1$ and $C > 0$, and constant matrix \vec{v} and \vec{v}' depending on R , such that $|\Theta_{(r)}^{(l)}(u, u') - \tilde{\pi}(G)^T (Rl\vec{v} + \vec{v}')| \leq C\alpha^l$. Furthermore, we denote the second largest eigenvalue of $A(G)$ and $\tilde{A}(G)$ as λ_2 and $\tilde{\lambda}_2$, respectively. Then, $\tilde{\lambda}_2 > \lambda_2$.*

Proof. According to the aggregation function for covariance matrix, we have

$$\begin{aligned} \vec{\Theta}^{(l)}(G) &= (1 - \delta)\mathcal{A}(G)\vec{\Theta}^{(l-1)}(G) + \delta\vec{\Theta}^{(l-1)}(G) \\ &= ((1 - \delta)\mathcal{A} + \delta I)\vec{\Theta}^{(l-1)}(G) = \tilde{\mathcal{A}}(G) \end{aligned}$$

The new aggregation matrix $\tilde{\mathcal{A}}(G)$ is a stochastic transition matrix as well, which can be seen from,

$$\sum_j \tilde{\mathcal{A}}(G)_{ij} = (1 - \delta) \sum_j \mathcal{A}(G)_{ij} + \delta \sum_j I_{ij} = 1$$

The new aggregation can slow down the convergence rate can seen from considering their eigenvalues. Suppose the eigenvalues of original matrix $\mathcal{A}(G)$ are $\{\lambda_1 > \lambda_2 > \dots > \lambda_{n^2}\}$. We already know that the maximum eigenvalue is $\lambda_1 = 1$, and the converge speed is governed by the second largest eigenvalue λ_2 . Now we consider the second largest eigenvalue $\tilde{\lambda}_2$ of matrix $\tilde{\mathcal{A}}$:

$$\tilde{\lambda}_2 = (1 - \delta)\lambda_2 + \delta = \lambda_2 + \delta(1 - \lambda_2) > \lambda_2$$

Since $\lambda_2 < \tilde{\lambda}_2 < 1$. Thus the convergence speed of residual GNTK will be slow down, through it is still exponential convergent. For the limit behavior of $\Theta_{(r)}^{(l)}(u, u')$ as l tends to infinity, we can directly use the proof strategy from Theorem 1. □

C.2 Residual connection in MLP

Theorem 3 (Convergence rate for GNTK with residual connection between transformations). *Consider a GNTK the form (8) and (12). If $\mathcal{A}(G)$ is irreducible and aperiodic, with a stationary distribution $\pi(G, G')$, then there exist constants $0 < \alpha < 1$ and $C > 0$, and constant matrix v and v' depending on R , such that, $|\Theta_{(r)}^{(l)}(u, u') - \bar{\pi}(G)^T \cdot (Rl(1 + \frac{\sigma_w^2}{2})^{Rl} \vec{v} + \vec{v}')| \leq C\alpha^l$.*

Proof. For residual connection in MLP, we have,

$$q_r(u) = q_{r-1}(u) + \frac{\sigma_w^2}{2} q_{r-1}(u) = (1 + \frac{\sigma_w^2}{2}) q_{r-1}(u)$$

Since $\frac{\sigma_w^2}{2} > 0$, $q_r(G)$ grows at an exponential rate.

Now, we turn to compute the correlation term $C_r(u, u')$. For convenience, we suppose $q_r(u) = q_r(u')$. Then,

$$\begin{aligned} C_{r+1}(u, u') &= \frac{\Sigma_{r+1}(u, u')}{q_{r+1}(u)} = \frac{1}{1 + \frac{\sigma_w^2}{2}} \frac{\Sigma_r(u, u')}{q_r(u)} + \frac{1}{1 + \frac{\sigma_w^2}{2}} \frac{\sigma_w^2}{2} f(C_r(u, u')) \\ &= \frac{1}{1 + \frac{\sigma_w^2}{2}} C_r(u, u') + \frac{\frac{\sigma_w^2}{2}}{1 + \frac{\sigma_w^2}{2}} f(C_r(u, u')) \end{aligned}$$

Using Taylor expansion of f near 1, as have been done in the proof of Lemma 2,

$$f(x)|_{x \rightarrow 1-} = x + \frac{2\sqrt{2}}{3\pi} (1-x)^{3/2} + O((1-x)^{5/2})$$

we have,

$$C_{r+1}(u, u') = C_r(u, u') + \frac{2\sqrt{2}}{3\pi} \frac{\frac{\sigma_w^2}{2}}{1 + \frac{\sigma_w^2}{2}} [(1 - C_r(u, u'))^{3/2} + O((1 - C_r(u, u'))^{5/2})]$$

Note that it is similar to the case of MLP without residual connection:

$$C_{r+1}(u, u') = C_r(u, u') + \frac{2\sqrt{2}}{3\pi} [(1 - C_r(u, u'))^{3/2} + O((1 - C_r(u, u'))^{5/2})]$$

Following the proof diagram in Lemma 3 and Theorem 1, we can obtain the behavior of $\Sigma_{(r)}^{(l)}(u, u')$ and $\Theta_{(r)}^{(l)}(u, u')$ in the large depth limit,

$$\begin{aligned} |\Sigma_{(r)}^{(l)}(u, u') - \bar{\pi}(G)^T ((1 + \frac{\sigma_w^2}{2})^{Rl} \vec{v})| &\leq C\alpha^l \\ |\Theta_{(r)}^{(l)}(u, u') - \bar{\pi}(G)^T (Rl(1 + \frac{\sigma_w^2}{2})^{Rl} \vec{v} + \vec{v}')| &\leq C\alpha^l \end{aligned}$$

□

D APPENDIX: Dataset and Experimental Implementation

D.1 Dataset

MUTAG [34] is a bioinformatics dataset; Cora, Citeseer and Pubmed [19] are commonly used citation network data for the node classification. We illustrate the detailed information for the three datasets as follows and summary can be found in Table 3.

- The Cora dataset consists of 2708 scientific publications classified into one of seven classes. The citation network consists of 5429 links. Each publication in the dataset is described by a 0/1-valued word vector indicating the absence/presence of the corresponding word from the dictionary. The dictionary consists of 1433 unique words.

- The Citeseer dataset consists of 3312 scientific publications classified into one of six classes. The citation network consists of 4732 links. Each publication in the dataset is described by a 0/1-valued word vector indicating the absence/presence of the corresponding word from the dictionary. The dictionary consists of 3703 unique words.
- The Pubmed Diabetes dataset consists of 19717 scientific publications from PubMed database pertaining to diabetes classified into one of three classes. The citation network consists of 44338 links. Each publication in the dataset is described by a TF/IDF weighted word vector from a dictionary which consists of 500 unique words.

Table 3: Details of Datasets

Dataset	Graphs	Nodes	Edges	Classes	Features	Avg. nodes	Critical Edge Sampling
MUTAG	188	-	-	2	-	17.9	-
Cora	1	2,708	5,429	7	1,433	-	24.94%
Citeseer	1	3,327	4,732	6	3,703	-	35.15%
Pubmed	1	19,717	44,338	3	500	-	22.23%

D.2 Experimental Implementation

We use the PyTorch implementation to simulate both infinite-width and finite-width GCNs:

- The **infinite-width** GCNs use part of code from [4] which is originally adopted for graph classification. We redesigned the calculation method of GNTK³ according to the formula in section 3.1 and used it to process node classification tasks.
- For **finite-width** GCNs⁴, we use the code from [33], we perform random hyper-parameter search for each model, and report the case giving the best accuracy on validation set of each benchmark, following the same strategy as [33]. The difference is that, in each experiment, we fix the edge sampling percent as $\rho = \frac{|V|}{2|E|}$, which listed in the last column of Table 3.

All the codes mentioned above use the MIT license. All experiments are conducted on with two Nvidia Quadro RTX 6000 GPUs.

E APPENDIX: Additional Experiment and Discussion

E.1 Infinite-Width Backbone

In the main text, we reported the performance of GCNs with finite-width, here we display more results with respect to infinite-width GCNs, as shown in Table 4. We apply Critical DropEdge to infinite-width backbone on node classification with a semi-supervised setting. We consider two backbones: GCN [19] and JKNet [40]. For the edge rate, we use the edge preserving percent as $\rho(G)$ which shown in Table 3. Table 4 summaries the performance on three citation network datasets. In

³We use the implementation of GNTK available at <https://github.com/KangchengHou/gntk> [4].

⁴We use the implementation of DropEdge available at <https://github.com/DropEdge/DropEdge> [33].

Table 4: Comparison results of test accuracy (%) with different infinite-width backbones.

Dataset	Backbone	4-layer		8-layer		32-layer		64-layer	
		Original	C-DropEdge	Original	C-DropEdge	Original	C-DropEdge	Original	C-DropEdge
Cora	GCN	79.98	79.98	79.48	80.61	73.75	75.86	72.59	74.03
	JKNet	78.27	77.29	80.26	80.02	78.00	79.01	75.90	76.75
Citeseer	GCN	66.38	66.97	54.42	64.88	50.72	51.22	43.77	46.49
	JKNet	67.04	67.67	65.54	66.45	54.57	56.39	46.71	47.96
Pubmed	GCN	74.59	74.77	73.58	76.67	71.63	74.77	66.28	71.72
	JKNet	75.30	74.35	76.42	77.17	75.71	76.68	74.81	75.74

this table, we report the performance of GCNs with 4/8/32/64 layers. It is shown that, in most cases, using Critical DropEdge (C-DropEdge) can achieve better results than original deep GNNs in the infinite-width case, especially when the model is deep.

E.2 Comparison to DropEdge

While our proposed Critical DropEdge shares the same program with the DropEdge method [33], we point out the main difference which can result in a corresponding advantage for our approach concerning the hyper-parameter search space. C-DropEdge has a fixed and graph-dependent edge preserving percent, which implies our hyper-parameter space is smaller than that of DropEdge. The edge preserving percent is one of the most significant hyper-parameter, which has a crucial influence on the final performance of the algorithm. In order to obtain good performance, DropEdge needs to spend a lot of effort to search on the space in terms of this hyper-parameter. In contrast, our method naturally determines the parameters, thus saving plenty of time. Whether from a theoretical perspective or from the final performance, the edge preserving percent we set is reasonable and effective.